HHS Public Access

Author manuscript

Cancer Res. Author manuscript; available in PMC 2019 January 15.

Published in final edited form as:

Cancer Res. 2018 January 15; 78(2): 422–435. doi:10.1158/0008-5472.CAN-17-1533.

HER2-driven Breast Tumorigenesis Relies upon Interactions of the Estrogen Receptor with Coactivator MED1

Yongguang Yang[1], **Marissa Leonard**[1,2], **Yijuan Zhang**[1], **Dan Zhao**[1], **Charif Mahmoud**[3], **Shugufta Khan**[4], **Jiang Wang**[4], **Elyse E. Lower**[3], and **Xiaoting Zhang**[1,2,*]

[1]Department of Cancer Biology, University of Cincinnati College of Medicine, Cincinnati, Ohio 45267, USA

[2]Graduate Program in Cancer and Cell Biology, University of Cincinnati College of Medicine, Cincinnati, Ohio 45267, USA

[3]Department of Internal Medicine, University of Cincinnati College of Medicine, Cincinnati, Ohio 45267, USA

[4]Department of Pathology and Laboratory Medicine, University of Cincinnati College of Medicine, Cincinnati, Ohio 45267, USA

Abstract

Studies of the estrogen receptor (ER) coactivator protein MED1 have revealed its specific roles in pubertal mammary gland development and potential contributions to breast tumorigenesis, based on co-amplification of MED1 and HER2 in certain breast cancers. In this study, we generated a mouse model of mammary tumorigenesis harboring the MMTV-HER2 oncogene and mutation of MED1 to evaluate its role in HER2-driven tumorigenesis. MED1 mutation in its ER-interacting LxxLL motifs was sufficient to delay tumor onset and impair tumor growth, metastasis and cancer stem-like cell formation in this model. Mechanistic investigations revealed that MED1 acted directly to regulate ER signaling through the downstream IGF-1 pathway but not the AREG pathway. Our findings show that MED1 is critical for HER2-driven breast tumorigenesis, suggesting its candidacy as a disease-selective therapeutic target.

INTRODUCTION

Estrogen receptor (ER) α is the key functional mediator of estrogen signaling and plays prominent roles in both normal mammary gland development and breast cancer (1, 2). Clinically, over 70% of breast cancers are ER α positive and estrogen signaling is a primary driver in promoting breast cancer initiation, progression and metastasis (2, 3). As a nuclear receptor superfamily member, ER has characteristic domains that include a N-terminal AF-1 activation domain, a highly conserved central DNA binding domain (DBD) and a conserved C-terminal ligand binding domain (LBD) that contains activation domain AF-2 (4, 5).

*Corresponding Author's Mailing Address: Xiaoting Zhang, Department of Cancer Biology, 3125 Eden Avenue, Cincinnati, OH 45267, Tel: 513-558-3017, Fax: 513-558-4454, zhangxt@ucmail.uc.edu.

DISCLOSURE OF POTENTIAL CONFLICTS OF INTEREST

No potential conflicts of interest were disclosed.

Ligand-bound ER acts through its AF-2 domain to recruit diverse transcriptional cofactors that facilitate RNA polymerase II general transcription machinery assembly and transcription of target genes (1, 4). Among these cofactors, Mediator complex has been recognized as the main hub for the direct interaction between ER and RNA polymerase II (6, 7).

Estrogen receptor interacts with the Mediator complex through directly binding to two classical LxxLL motifs of the Mediator subunit 1 (MED1) (8, 9). Thus, knockdown of MED1 expression abolishes the expression of ERα-dependent genes, but does not affect the target gene expression of other transcription factors such as p53 that interact with another Mediator subunit (4). We have recently generated a MED1 mutant knockin ($MED1^{KI/KI}$) mouse model with mutations in both of the ER-interacting LxxLL motifs of MED1 (10). It was found that mutation of MED1 *in vivo* did not affect the overall fertility and survival of the mice. Instead, it played a tissue-, cell-, and gene-specific role in mediating ER functions in pubertal mammary gland development, but not the development of other estrogen-responsive tissues such as uterus and bone (10). Furthermore, we found that MED1 is selectively expressed in luminal but not basal mammary epithelial cells and that MED1 LxxLL motifs play a key role in the mammary luminal progenitor cell formation and differentiation (10).

MED1 is over-expressed in a high proportion (~40%–50%) of primary breast cancers and breast cancer cell lines (11, 12). Importantly, the MED1 gene is located in the chromosome *17q12* region, also known as the HER2 amplicon, and co-amplifies with HER2 in almost all instances in breast cancer (11, 12). The HER2/neu receptor is an EGF family transmembrane tyrosine kinase that is amplified and overexpressed in 20%–30% of breast cancer (13). We have recently further confirmed that a high level of MED1 protein expression strongly correlated with HER2+ status using a human breast cancer tissue microarray (14). Importantly, our research further established MED1 as a key crosstalk point for the HER2 and ER pathways in mediating anti-estrogen resistance of HER2+/ER+ human breast cancer cells (14). Consistent with the above mentioned role for MED1 in luminal progenitor cell formation, MMTV-HER2 mammary tumors are also thought to originate from luminal progenitor cells (15, 16). However, despite these evidences, whether MED1 and its LxxLL motifs play a role in HER2-driven breast tumorigenesis still remains unknown.

To test this, we have crossed the $MED1^{KI/KI}$ mice with a MMTV-HER2 transgenic mouse model to generate MMTV-HER2/$MED1^{KI/KI}$ mice. We found that MED1 LxxLL motif mutations led to a significantly delayed onset and impaired growth and lung metastasis of MMTV-HER2 tumors. Consistent with these, we found significantly decreased cell proliferation, angiogenesis and cancer stem cell (CSC) formation by the MED1 mutations. Further mechanistic studies were carried out to determine the molecular pathways underlying MED1 functions in these processes and these findings were confirmed using both human breast cancer cell line and patient samples. Overall, our data support a key role for MED1 LxxLL motifs in HER2-driven mammary tumorigenesis and its potential use as a tissue-specific target for the treatment of HER2+/ER+ breast cancer.

MATERIALS AND METHODS

Transgenic mice

MED1 LxxLL motif mutant knockin (MED1$^{KI/KI}$) mice have been previously described (10) and were crossed to FVB background through F10 before crossing to MMTV-HER2 mice. MMTV-HER2 (17) and NOD-SCID mice were purchased from The Jackson Laboratory. To monitor primary mammary tumor formation, manual palpation was performed weekly and the tumor volume was calculated by the formula: volume = length × width^2 /2. Tumor-free survival was analyzed using the Kaplan-Meier method. All animals were housed in AAALAC-approved facilities at the University of Cincinnati. All procedures were approved by IACUC and in accordance with the NIH guidelines as in the Guide for Care and Use of Laboratory Animals.

Mammosphere formation, Transwell and 3D culture assays

For the mammosphere formation assay, 3 × 10^4 cells were seeded into each well of ultra-low adhesion 24-well plates (Coring) in DMEM/F-12 (1:1) medium (Corning) containing 0.4% BSA (Fisher BioReagents), Insulin (5 ng/ml, Sigma), B-27 (50×, Invitrogen), EGF (20 ng/ml, R&D) and bFGF (10 ng/ml, R&D) and 1% Penicillin/Streptomycin (Fisher BioReagents). Mammospheres were imaged 7–10 days after initiation of culture and analyzed using Zeiss Axiovision software (Carl Zeiss, Jena, Germany). For invasion and migration assays, 5 × 10^4 serum-starved tumor cells were suspended with 100 μl serum-free medium and plated in 8 μm pore Transwell inserts (Corning, NY) in a 24-well plate format with or without 100 μl Matrigel (Corning, 1:10 diluted in DMEM), respectively. The lower compartment was filled with 700 μl medium containing 10% FBS and cultured for 18 hrs. Cells were then fixed and stained in 20% methanol containing 1% crystal violet for 10 min. Tumor cell 3D culture was conducted essentially as described in (18). Briefly, 100 μl of Matrigel was spread evenly with a pipette tip on the surface of pre-chilled 24-well plate and incubated at 37°C for 30 min to allow the Matrigel to gel. 5× 10^3 cells were suspended in 600 μl mammosphere culture medium with 5% Matrigel, added onto the pre-coated surface and cultured for 14 days with the medium changed every 4 days.

Orthotopic tumor xenograft and OSI-906 treatment

For orthotopic tumor xenograft experiments, flow cytometry sorted CSC-enriched cells were suspended with PBS and mixed with Matrigel (1:1) to a final volume of 100 μl. The mixture was injected into the fourth mammary fat pads of NOD-SCID as described (19). Tumor sizes were measured with calipers weekly as above and the frequencies of TICs in limiting dilution assays were calculated through the following website: http://bioinf.wehi.edu.au/software/elda/. IGF-1 receptor inhibitor OSI-906 (LC Laboratories) was dissolved in dimethyl sulfoxide (DMSO) at 10mM and stored at −20°C. For OIS-906 treatment, when the tumor volume reached 600 mm^3, mice were randomly assigned to vehicle (25mM tartaric acid (Sigma) in water) or OSI-906 (50 mg/kg) treatments by oral gavage once a day for 14 days. At the end of treatment, tumors were collected for flow cytometry analysis, mammosphere culture assays as well as paraffin/frozen sections for immunostaining analysis.

Conditioned medium, HUVECs tube formation and Matrigel plug assays

1×10^7 cells from MMTV-HER2/MED1$^{+/+}$ or MMTV-HER2/MED$^{KI/KI}$ primary tumors were plated onto a 10cm cultured dish and cultured in DMEM medium containing 10% serum for 24 hours. Culture medium was then changed to DMEM medium (high glucose) containing 1% FBS and cultured for another 24 hours. The medium was collected and centrifuged at 1000 × g for 5 min to remove the debris. For tube formation assay *in vitro*, human umbilical vein endothelial cells (HUVECs) were cultured in M199 medium containing 1% FBS for 5 hours and then digested with trypsin and re-suspended with conditioned or control medium. The cells were seeded onto Matrigel coated 96-well plate at 6×10^4 cells per well in 100 μl volume and cultured for 6–18 hours before imaging. For blood vessel formation in Matrigel plug *in vivo*, 200 μl of the above described conditioned or control medium was mixed with 300 μl Matrigel (total 500 μl) and injected subcutaneously into the flank of nude mice. The mice were maintained for 10 days before the Matrigel plugs were recovered for analyses.

Human Breast Cancer Tissue Samples

The human breast cancer specimens were collected with written informed consent from the patients at the University of Cincinnati Cancer Institute (UCCI) Breast Cancer Center of Excellence. The studies were conducted in accordance with the ethical guidelines stated in the Declaration of Helsinki under the protocol #09-04-14-02 approved by the Institutional Review Board (IRB) of the University of Cincinnati.

Statistical Analysis

All experiments were repeated at least 3–5 times and data was expressed as average ± SD. Statistical analyses of the data were performed by pairwise Student's *t* test. It is considered statistically significant (*) if $P \leq 0.05$ and very significant (**) if $P \leq 0.01$. Kaplan-Meier tumor free survival data were compared using the log-rank test. Tumor number and metastatic lesions were statistically analyzed using GraphPad software with two-tailed Student t tests.

RESULTS

MED1 LxxLL motifs play critical roles in HER2+ mammary tumor onset, growth and metastasis

To examine the role of MED1 LxxLL motifs in HER2-mediated mammary tumorigenesis, we crossed MED1$^{KI/KI}$ mice with MMTV-HER2 mice to generate control MMTV-HER2/MED1$^{+/+}$ and MMTV-HER2/MED1$^{KI/KI}$ mice (Fig 1A). Interestingly, we observed a significantly delayed tumor onset in MMTV-HER2/MED1$^{KI/KI}$ mice (~16 weeks later on average) when compared to that of MMTV-HER2/MED1$^{+/+}$ control mice (Fig 1B–C). While all MMTV-HER2/MED1$^{+/+}$ mice form tumors within 65 weeks, roughly10–15% of the MMTV-HER2/MED1$^{KI/KI}$ mice did not produce any palpable tumors even during the whole 2-year observation period. Furthermore, tumors in MMTV-HER2/MED1$^{KI/KI}$ mice grow much slower and had lower tumor weight at the time of collection (~2 months after palpation of primary tumor) when compared to those of controls (Fig 1D–F). Moreover, H&E staining of the serial lung sections from tumor bearing mice demonstrated a reduced

number of tumor metastatic lesions in MMTV-HER2/MED1$^{KI/KI}$ mice when compared with that of controls (Fig 1G–H). Taken together, these data support a critical role for MED1 LxxLL motifs in mediating HER2+ mammary tumor onset, growth and metastasis.

MMTV-HER2/MED1$^{KI/KI}$ mammary tumors exhibited decreased cell proliferation, increased necrosis and impaired ER target gene expression

To examine whether the decreased tumor growth observed in MMTV-HER2/MED1$^{KI/KI}$ mice is due to reduced tumor cell proliferation or enhanced cell death/apoptosis, we carried out the IHC staining using antibodies against Ki67 and cleaved caspase-3, respectively. We found that the number of proliferating cells in MMTV-HER2/MED1$^{KI/KI}$ tumors were dramatically decreased (Fig 2A, left panel and Figure 2B, upper panel), but the cleaved caspase-3 protein positive apoptotic cells were not increased in MMTV-HER2/MED1$^{KI/KI}$ tumors (Fig 2A, right panel and Figure 2B, lower panel). Histological analysis by H&E staining further revealed that there are widely distributed necrotic lesions in MMTV-HER2/MED1$^{KI/KI}$ tumors but not in MMTV-HER2/MED1$^{+/+}$ controls (Fig S1A). Mechanistically, as a control we found that the expression of ERα, PR, MED1 and HER2 proteins is not changed by western blots analyses (Fig 2C). However, the expression of both well-known traditional ER target genes (e.g. IGF-1 (20, 21) and Cyclin D1 (22)) and the newly identified EGF/HER2 pathway-activated ER target genes (e.g. LIF and ACP6) (14, 23) were all dramatically reduced in MMTV-HER2/MED1$^{KI/KI}$ tumors (Fig 2D). To further determine whether the mutation of MED1 LxxLL motifs directly impairs the expression of these ERα target genes through affecting the recruitment of RNA polymerase II, we then examined the chromatin occupancy of MED1 and RNA polymerase II on their promoters. Indeed, chromatin immunoprecipitation (ChIP) analysis indicated that the presence of both MED1 and RNA polymerase II on the promoter of *TFF1, IGF-1* and *AREG* genes was significantly reduced in MMTV-HER2/MED1$^{KI/KI}$ tumor cells (Fig 2E–F). These findings support that the MED1 LxxLL motifs play a critical role in MMTV-HER2 tumor cell proliferation through direct regulation of both traditional and EGF/HER2-activated ERα target gene expression.

MED1 LxxLL motif mutations impair migration, invasion and EMT of MMTV-HER2 tumors

Since reduced tumor lung metastasis was observed in MMTV-HER2/MED1$^{KI/KI}$ mice (Fig 1G–H), we decided to analyze the migration and invasion capabilities of these tumor cells through transwell assays *in vitro* (Fig 3A, left two panels). Statistic results clearly showed that the number of migrated and invaded cells in the MMTV-HER2/MED1$^{KI/KI}$ group were significantly lower than that in MMTV-HER2/MED1$^{+/+}$ controls (Fig 3B). Moreover, when cultured in 3D Matrigel, we observed MMTV-HER2/MED1$^{+/+}$ tumor cells but not MMTV-HER2/MED1$^{KI/KI}$ cells had migrated out from the original colonies and invaded into the surrounding matrix (Fig 3A, right panel). Because epithelial-mesenchymal transition (EMT) has been shown to play a key role in promoting tumor cell metastasis (24), we then analyzed the expression of EMT-related genes in MMTV-HER2/MED1$^{KI/KI}$ and MMTV-HER2/MED1$^{+/+}$ tumor cells using realtime RT-PCR (Fig 3C). Notably, we found the expression of a number of these genes, including *twis*t, *snail* and *slug,* were significantly downregulated in the MMTV-HER2/MED1$^{KI/KI}$ tumors. Further immunofluorescence staining (Fig 3D) and immunoblot (Fig 3E) results confirmed the increased E-cadherin and decreased Vimentin

and N-cadherin expression in these tumors. In addition, we found that the expression of matrix metalloproteinases 9 (MMP9) (25, 26) but not *MMP2* or *MMP7* was significantly inhibited in MMTV-HER2/MED1$^{KI/KI}$ tumors (Fig 3E–F). Taken together, these data support the conclusion that the MED1 LxxLL motif mutations affect MMTV-HER2 tumor cell migration and invasion capabilities through controlling the expression of genes involved in EMT and ECM degradation.

MED1 LxxLL motif mutations reduced MMTV-HER2 tumor angiogenesis

Since angiogenesis plays a critical role in both cancer cell proliferation and metastatic spread and loss of angiogenesis is linked to tumor necrosis (27), we next decided to evaluate the angiogenesis in these tumors by immunostaining using an antibody against blood vessel endothelial marker CD31 (Fig 4A). Our results clearly demonstrated that the CD31-positive cells in MMTV-HER2/MED1$^{KI/KI}$ tumors were greatly reduced when compared with that of MMTV-HER2/MED1$^{+/+}$ control tumors (Fig 4B). Furthermore, we carried out *in vitro* blood vessel formation assays by using conditioned medium from cultured MMTV-HER2/MED1$^{+/+}$ and MMTV-HER2/MED1$^{KI/KI}$ tumor cells (Fig 4C). Consistent with above results, the conditioned medium from MMTV-HER2/MED1$^{KI/KI}$ tumor cells induced tube formation of HUVECs to a significantly reduced extent (Fig 4D). Moreover, we tested the ability of the conditioned media to induce microvessel formation *in vivo* by a Matrigel plug angiogenesis assay (Fig 4E). 10 days after embedding, we could clearly see the formed vessels filled with red blood cells in the Matrigel plugs with conditioned medium from MMTV-HER2/MED1$^{+/+}$ tumor cells, while there were very little or no blood vessels in the Matrigel plug containing conditioned medium from MMTV-HER2/MED1$^{KI/KI}$ tumor cells or PBS control (Fig 4E). Vascularization in the Matrigel plugs was further confirmed by CD31 staining of frozen sections of the plugs (Fig 4F). The results confirmed that the percentage of CD31-positive area in the Matrigel plug containing MMTV-HER2/MED1$^{KI/KI}$ conditioned medium is significantly lower than that in MMTV-HER2/MED1$^{+/+}$ controls (Fig 4G). To analyze whether the reduced blood formation is due to decreased VEGF (28) expression in MMTV-HER2/MED1$^{KI/KI}$ tumors, we carried out western blot analysis (Fig 4H) and found a dramatically decreased VEGFA protein expression in the MMTV-HER2/MED1$^{KI/KI}$ tumors when compared with that from MMTV-HER2/MED1$^{+/+}$ controls (Fig 4H–I). Taken together, these results indicated that MED1 LxxLL motif mutations reduced tumor blood vessel formation most likely through downregulation of VEGFA expression.

MMTV-HER2/MED1$^{KI/KI}$ tumors have impaired CSC functions both *in vitro* and *in vivo*

Since MED1 LxxLL motifs play a role in luminal progenitor cell formation during development, we next examined whether CSCs (29, 30) are affected in the MMTV-HER2/MED1$^{KI/KI}$ tumors. Our flow cytometry analyses indicated that the Lin^{-}CD24^{+}CD29^{hi} CSCs-enriched population was significantly reduced in MMTV-HER2/MED1$^{KI/KI}$ tumors when compared with that in MMTV-HER2/MED1$^{+/+}$ controls ($p < 0.05$) (Fig 5A–B) (15, 31). The sorted cells from each group were further cultured for mammosphere formation assays (Fig 5C). Again, our results clearly showed that both the size and number of the mammospheres formed by MMTV-HER2/MED1$^{KI/KI}$ cells were significantly reduced (Fig 5D–E). We next carried out limited dilution assays by orthotopically xenografting Lin^{-}CD24^{+}CD29^{+} cells from MMTV-HER2/MED1$^{+/+}$ and MMTV-HER2/MED1$^{KI/KI}$ tumors

into NOD-SCID recipient mice (Fig 5F). We found that MED1 LxxLL motif mutations in CSCs significantly compromised their tumorigenicity in an autonomous manner. While 1 in 88.2 $Lin^{-}CD24^{+}CD29^{+}$ MMTV-HER2/$MED1^{+/+}$ tumor cells forms a tumor, only about 1 out of 525.6 $Lin^{-}CD24^{+}CD29^{+}$ MMTV-HER2/$MED1^{KI/KI}$ tumor cells was able to do so (Fig 5G). FACS analysis further showed the CSC populations in MMTV-HER2/$MED1^{KI/KI}$ grafted tumors were significantly lower than that in MMTV-HER2/$MED1^{+/+}$ grafted tumors (Fig 5H–I). IHC staining confirmed that the percentage of Ki67-positive proliferating cells was also significantly lower in grafted MMTV-HER2/$MED1^{KI/KI}$ tumors (Fig S1B–C). Consistent with Fig 2C–D, western blot and realtime RT-PCR analyses confirmed decreased ERα target gene expression in the MMTV-HER2/$MED1^{KI/KI}$ graft tumors when compared with that of controls (Fig S1D–E). Collectively, these results support that MED1 LxxLL motif-mediated signaling plays a critical intrinsic role in regulating MMTV-HER2 CSC formation and functions.

IGF-1 pathways play a key role in mediating MED1 functions during both normal development and tumorigenesis

We have found the expression of a number of ER target genes in both normal mammary gland and tumor are affected by MED1 LxxLL motif mutations (Fig 2D and S2A) (10). Among them, knockout of Amphiregulin (AREG) and IGF-1 exhibited a very similar mammary gland development phenotype as $MED1^{KI/KI}$ mice (32, 33). To examine whether one or both pathways are important in mediating the above MED1 functions, we carried out rescue experiments by implanting slow releasing pellets containing AREG (5 μg/pellet) or IGF-1(5 μg/pellet) in the 4^{th} mammary glands of 4week old $MED1^{KI/KI}$ mice (Fig S2B). We found the development of $MED1^{KI/KI}$ mammary glands was fully recovered by IGF-1-containing but not AREG-containing pellets in terms of the number of terminal end buds (TEB), percentage of ductal occupancy and the number of tertiary branches (Fig S2C–E). Flow cytometry analyses further showed that the percentage of $Lin^{-}CD24^{+}CD29^{hi}$, $Lin^{-}CD24^{+}CD29^{Med}$ and $Lin^{-}CD29^{+}Scal^{+}$ cell populations were all restored to the wild type levels by the IGF-1-containing pellet (Fig S2F–G).

Based on these findings, we further examined the IGF-1 and its downstream signaling pathways in the MMTV-HER2/$MED1^{KI/KI}$ tumors. The results clearly showed that IGF-1 protein level was significantly reduced in MMTV-HER2/$MED1^{KI/KI}$ tumors when compared with that of MMTV-HER2/$MED1^{+/+}$ controls (Fig 6A). Although the total IGF-1R protein level was not changed, its phosphorylation and the phosphorylation of AKT and mTOR were significantly downregulated in MMTV-HER2/$MED1^{KI/KI}$ tumors. To further test the function of IGF-1 in MMTV-HER2/$MED1^{KI/KI}$ tumor cells *in vitro*, we supplemented recombinant IGF-1 in the culture medium and performed mammosphere assays (Fig 6B). The results showed that addition of IGF-1 could fully restore the number and size of mammospheres formed and the $CD24^{+}CD29^{hi}$ CSC-enriched population to wild type levels (Fig 6C–E). In addition, IGF-1 is able to restore the migration and invasion capabilities of MMTV-HER2/$MED1^{KI/KI}$ tumor cells in transwell and 3D culture assays (Fig 6F–I). These data support a key role for IGF-1 pathways in mediating MED1 LxxLL motif functions during both normal mammary gland development and tumorigenesis.

Inhibition of IGF-1R phenocopies MED1 LxxLL motif mutations in both mouse and human HER2+ cancer cells

To further test the role of the IGF-1 signaling pathway in MMTV-HER2 tumorigenesis *in vivo*, MMTV-HER2/MED1$^{+/+}$ and MMTV-HER2/MED1$^{KI/KI}$ tumor cells were transplanted into nude mice and treated with vehicle control or IGF-1 receptor inhibitor OSI-906. We found that OSI-906 treatment could significantly slow the growth of grafted MMTV-HER2/MED1$^{+/+}$ tumors just like MED1 LxxLL motif mutations (Fig 7A and S3A). Flow cytometry analyses further demonstrated similar levels of Lin^{-}CD24^{+}CD29^{hi} CSCs populations in both OSI-906 treated MMTV-HER2/MED1$^{+/+}$ and vehicle treated MMTV-HER2/MED1$^{KI/KI}$ grafted tumors (Fig 7B). In addition, similarly to what we observed in the MMTV-HER2/MED1$^{KI/KI}$ tumors, we found a reduced number of Ki67- and CD31-positive cells, as well as increased tumor necrosis in OSI-906 treated MMTV-HER2/MED1$^{+/+}$ tumor groups (Fig 7C–F and Fig S3B), but the caspase 3-positive cells were still not affected (Fig S3C). Immunoblotting results confirmed that although the protein level of IGF-1 remains to be high, the activation of the IGF-1 signaling downstream components of pIGF-1R, pAKT and pmTOR was significantly reduced in OSI-906 treated MMTV-HER2/MED1$^{+/+}$ tumors to a level comparable to that of the vehicle treated MMTV-HER2/MED1$^{KI/KI}$ tumors (Fig S3D). In addition, there was a significant decrease in the expression of VEGFA in MMTV-HER2/MED1$^{+/+}$ by OSI-906 treatments. We next further examined the importance of IGF-1 signaling in HER2+/ER+ human breast cancer cells and found that inhibition of IGF-1R with OSI-906 could significantly reduce the migration and invasion, mammosphere formation as well as CSCs population of BT474 *in vitro* (Fig S4A–H). We have also performed IHC staining of the expression of MED1 and IGF-1 proteins using human breast cancer clinical samples (see Table S1 for patient demographic information). As shown in Fig 7G, the results clearly indicate that there is a very significant ($p < 0.001$) positive correlation between MED1 and IGF-1 protein levels (Fig 7H). Collectively, these data support a key role for MED1 regulation of the IGF-1 pathway in HER2+ tumor formation.

DISCUSSION

Our previous generation of MED1 LxxLL motif mutant knockin mice revealed its tissue-specific role during pubertal mammary gland development by affecting luminal progenitor cell formation and differentiation (10). In this study, we further determined its role and underlying molecular mechanism in breast tumorigenesis and found that: (i) MED1 LxxLL motif mutations cause a significantly delayed MMTV-HER2 mammary tumor onset with decreased tumor growth and lung metastasis; (ii) MED1 LxxLL motif mutations significantly inhibit MMTV-HER2 tumor cell proliferation and ER target gene expression; (iii) CSC formation, tumor cell EMT and metastatic capabilities of MMTV-HER2 tumors are impaired by MED1 mutations; (iv) MED1 regulation of IGF-1 plays a key role in the above observed phenotypes during both mammary gland development and tumorigenesis; (v) inhibition of the IGF-1 pathway significantly reduces the metastatic capability and CSC formation of human breast cancer cells; and (vi) MED1 and IGF-1 co-express in a large cohort of human breast cancer patient samples.

Taken together, these data revealed a key role of MED1 and its LxxLL motifs in breast tumorigenesis *in vivo* through affecting a plethora of processes such as cell proliferation, metastasis, cancer stem cell formation and angiogenesis. This is significant because MED1 is known to be overexpressed in a high percentage (40–50%) of human breast cancer and co-amplify with HER2 in almost all instances (11, 12). Although the HER2 amplicon has been well studied, there is currently no information about whether any of the genes that co-amplify with HER2 play a role in HER2-driven tumorigenesis. We have previously shown a direct crosstalk between HER2 and MED1 in mediating anti-estrogen resistance (14), and a recent study has identified an increased MED1 mutation in circulating tumor cells of human patients after anti-estrogen and anti-HER2 therapies (34). Analyses of provisional TCGA and METABRIC datasets further indicate that high MED1 expression correlates with HER2-amplification, larger tumor size, lymph node positive status, higher tumor grades and poor patient survival (Fig S5A–I). Although whether MED1 overexpression playing a driving or synergistic role with HER2 in these processes still needs to be investigated in the future, here we have provided further evidence indicating a critical role for MED1 in HER2-mediated breast tumorigenesis *in vivo*. Importantly, we have further confirmed the key findings of this study using both human breast cancer cell lines and patient samples.

CSCs are considered to be the driving force for both tumor initiation and metastasis to other organs (35). We have already found mammary stem/progenitor cell populations were significantly decreased in the MED1$^{KI/KI}$ mammary glands. Interestingly, MED1 is specifically expressed in luminal mammary epithelial cells and MED1 LxxLL motif mutations led to a decreased Lin^{-}CD24^{+}CD29^{hi} mammary stem cell-enriched population and Lin^{-}CD29^{+}Scal^{+} luminal progenitor cells. Current studies support that MMTV-HER2 tumors are originated from luminal progenitor cells (15, 16). Initially, these tumors are largely ER+ (albeit heterogeneous), with gradual loss of ERα expression later, while the tumors maintain growth dependence on and respond to estrogen stimulation (16). Here, we have provided further evidences supporting a role for MED1 LxxLL motifs in cancer stem cell formation of MMTV-HER2 tumors. First, we observed a decreased Lin^{-}CD24^{+}CD29^{hi} CSCs population in MMTV-HER2/MED1$^{KI/KI}$ tumors when compared with that from MMTV-HER2/MED1$^{+/+}$ controls. Second, our *in vitro* analyses demonstrated that MMTV-HER2/MED1$^{KI/KI}$ tumors have reduced stem cell content and mammosphere formation capabilities. Third, our *in vivo* limiting dilution assays showed that the number of tumor initiating cells (TIC) was significantly decreased from 1 in 88.2 in MMTV-HER2/MED1$^{+/+}$ tumors to 1 in 526.5 in MMTV-HER2/MED1$^{KI/KI}$ tumors. Together, these data indicated a critical role for MED1 LxxLL motifs in both mammary stem/progenitor cell and cancer stem cell formation not only *in vitro* but also *in vivo*.

It is recognized that estrogen and progesterone are the key hormones regulating mammary stem/progenitor cell formation during both normal development and tumor formation (36–38). Although recent studies have identified the role of progesterone in the regulation of mammary stem/progenitor cells through the RANKL pathway, the downstream signaling pathway through which estrogen exerts its function remains to be elucidated (37, 39, 40). Recent studies have established insulin growth factor 1 (IGF-1) and amphiregulin (AREG) as major ERα downstream target genes mediating its function during pubertal mammary gland development (41, 42). Knockout of these genes in mice resulted in pubertal mammary

duct growth and mammary epithelial cell proliferation defects similar to that of MED1$^{KI/KI}$ mice (33, 43). Interestingly, we found that supplementation of exogenous IGF-1 but not AREG can fully rescue the pubertal mammary gland developmental defects of MED1$^{KI/KI}$ mice. Addition of IGF-1 was able to restore the affected Lin^{-}CD24^{+}CD29^{hi}, Lin^{-}CD24^{+}CD29^{Med} and Lin^{-}CD29^{+}Scal^{+} cell populations in MED1$^{KI/KI}$ mammary gland back to the wild type levels. Further, we found that IGF-1 can rescue the mammosphere formation capabilities of MMTV-HER2/MED1$^{KI/KI}$ tumor cells while inhibition of the IGF-1 pathway impairs cancer stem cell formation in both human and mouse tumor cells. We also observed a significant correlation of the expression of MED1 and IGF-1 proteins in human breast cancer patient samples. Although we cannot exclude that MED1 may still function through additional pathways to regulate mammary gland development and tumorigenesis, our study does support a critical role for the MED1/IGF-1 axis in these processes.

Clinically, IGF-1/IGF-1R correlates with HER2+/ER+ luminal human breast cancer and dysregulated IGF-1 signaling has also been implicated in breast cancer tumorigenesis and treatment resistance (44, 45). However, despite efforts to develop IGF-1 inhibitors for cancer therapies in the past decades and early success, there are significant setbacks due to limited effectiveness in late-stage clinical trials. Besides high toxicity and side effects (46), the reasons behind this could also include lack of predictive biomarkers for patient selection, IGF-1 activation through alternative downstream pathways such as insulin receptor (InsR), polymorphism of IGF-1 signaling components (47), the inclusion of high proportion of patients with stage IV disease in the trials (48), etc. Our finding of IGF-1 as a major MED1 downstream target in affecting mammary tumorigenesis *in vivo* provided a potentially new avenue to target this pathway for breast cancer treatment. In addition, targeting MED1 and its LxxLL motifs could also affect additional pathways that might be important for breast tumorigenesis. Indeed, we have shown that those EGF/HER2-regulated ER target genes such as ACP6 and LIF that are known to promote cell proliferation and are overexpressed in HER2+ human breast cancer were also down regulated by MED1 LxxLL motif mutations (23). We have also shown that MED1 LxxLL motifs play a rather tissue-, cell- and gene-specific role in pubertal mammary gland development but not the development of other tissues. Thus, future development of new innovative strategies to specifically target MED1 and its LxxLL motifs could be advantageous in both maximizing therapeutic efficacy and minimizing unwanted side effects. Given the fact that MED1 is overexpressed not only in HER2+ tumors (11, 12), such treatment strategies may also have a more broad application for other subtypes of breast cancer.

Supplementary Material

Refer to Web version on PubMed Central for supplementary material.

Acknowledgments

This study was supported by: Ohio Cancer Research Seed Money, Cincinnati Cancer Center and University of Cincinnati Cancer Institute Pilot Grants, Ride Cincinnati Award, Komen for the Cure Foundation Career Catalyst Grant (KG110028), American Cancer Society Research Scholar Grant (RSG-12-268-01) and National Institutes of Health Grant R01CA197865 (to X. Zhang). We thank B. Ehmer and G. Doerman for technical and editorial

support, respectively. We also thank The Cancer Genome Atlas (TCGA) and the Molecular Taxonomy of Breast Cancer International Consortium (METABRIC) for the invaluable clinical data.

References

1. Heldring N, Pike A, Andersson S, Matthews J, Cheng G, Hartman J, et al. Estrogen receptors: how do they signal and what are their targets. Physiol Rev. 2007; 87:905–31. [PubMed: 17615392]
2. Yager JD, Davidson NE. Estrogen carcinogenesis in breast cancer. N Engl J Med. 2006; 354:270–82. [PubMed: 16421368]
3. Saha Roy S, Vadlamudi RK. Role of estrogen receptor signaling in breast cancer metastasis. Int J Breast Cancer. 2012; 2012:654698. [PubMed: 22295247]
4. Zhang X, Krutchinsky A, Fukuda A, Chen W, Yamamura S, Chait BT, et al. MED1/TRAP220 exists predominantly in a TRAP/ Mediator subpopulation enriched in RNA polymerase II and is required for ER-mediated transcription. Mol Cell. 2005; 19:89–100. [PubMed: 15989967]
5. Tsai MJ, O'Malley BW. Molecular mechanisms of action of steroid/thyroid receptor superfamily members. Annu Rev Biochem. 1994; 63:451–86. [PubMed: 7979245]
6. Roeder RG. Lasker Basic Medical Research Award. The eukaryotic transcriptional machinery: complexities and mechanisms unforeseen. Nat Med. 2003; 9:1239–44. [PubMed: 14520363]
7. Malik S, Roeder RG. Transcriptional regulation through Mediator-like coactivators in yeast and metazoan cells. Trends Biochem Sci. 2000; 25:277–83. [PubMed: 10838567]
8. Kang YK, Guermah M, Yuan CX, Roeder RG. The TRAP/Mediator coactivator complex interacts directly with estrogen receptors alpha and beta through the TRAP220 subunit and directly enhances estrogen receptor function in vitro. Proc Natl Acad Sci U S A. 2002; 99:2642–7. [PubMed: 11867769]
9. Ren Y, Behre E, Ren Z, Zhang J, Wang Q, Fondell JD. Specific structural motifs determine TRAP220 interactions with nuclear hormone receptors. Molecular and Cellular Biology. 2000; 20:5433–46. [PubMed: 10891484]
10. Jiang P, Hu Q, Ito M, Meyer S, Waltz S, Khan S, et al. Key roles for MED1 LxxLL motifs in pubertal mammary gland development and luminal-cell differentiation. Proc Natl Acad Sci U S A. 2010; 107:6765–70. [PubMed: 20351249]
11. Zhu Y, Qi C, Jain S, Le Beau MM, Espinosa R 3rd, Atkins GB, et al. Amplification and overexpression of peroxisome proliferator-activated receptor binding protein (PBP/PPARBP) gene in breast cancer. Proc Natl Acad Sci U S A. 1999; 96:10848–53. [PubMed: 10485914]
12. Luoh SW. Amplification and expression of genes from the 17q11 approximately q12 amplicon in breast cancer cells. Cancer Genet Cytogenet. 2002; 136:43–7. [PubMed: 12165450]
13. Yarden Y. Biology of HER2 and its importance in breast cancer. Oncology. 2001; 61(Suppl 2):1–13.
14. Cui J, Germer K, Wu T, Wang J, Luo J, Wang SC, et al. Crosstalk Between HER2 and MED1 Regulates Tamoxifen Resistance of Human Breast Cancer Cells. Cancer Res. 2012; 72:5625–34. [PubMed: 22964581]
15. Visvader JE. Keeping abreast of the mammary epithelial hierarchy and breast tumorigenesis. Genes Dev. 2009; 23:2563–77. [PubMed: 19933147]
16. Shyamala G, Chou YC, Cardiff RD, Vargis E. Effect of c-neu/ErbB2 expression levels on estrogen receptor alpha-dependent proliferation in mammary epithelial cells: implications for breast cancer biology. Cancer Res. 2006; 66:10391–8. [PubMed: 17079459]
17. Guy CT, Webster MA, Schaller M, Parsons TJ, Cardiff RD, Muller WJ. Expression of the neu protooncogene in the mammary epithelium of transgenic mice induces metastatic disease. Proc Natl Acad Sci U S A. 1992; 89:10578–82. [PubMed: 1359541]
18. Lee GY, Kenny PA, Lee EH, Bissell MJ. Three-dimensional culture models of normal and malignant breast epithelial cells. Nat Methods. 2007; 4:359–65. [PubMed: 17396127]
19. Pece S, Tosoni D, Confalonieri S, Mazzarol G, Vecchi M, Ronzoni S, et al. Biological and molecular heterogeneity of breast cancers correlates with their cancer stem cell content. Cell. 2010; 140:62–73. [PubMed: 20074520]

20. Torres-Arzayus MI, Font de Mora J, Yuan J, Vazquez F, Bronson R, Rue M, et al. High tumor incidence and activation of the PI3K/AKT pathway in transgenic mice define AIB1 as an oncogene. Cancer Cell. 2004; 6:263–74. [PubMed: 15380517]
21. Smith LE, Shen W, Perruzzi C, Soker S, Kinose F, Xu X, et al. Regulation of vascular endothelial growth factor-dependent retinal neovascularization by insulin-like growth factor-1 receptor. Nat Med. 1999; 5:1390–5. [PubMed: 10581081]
22. Musgrove EA, Lee CS, Buckley MF, Sutherland RL. Cyclin D1 induction in breast cancer cells shortens G1 and is sufficient for cells arrested in G1 to complete the cell cycle. Proceedings of the National Academy of Sciences of the United States of America. 1994; 91:8022–6. [PubMed: 8058751]
23. Lupien M, Meyer CA, Bailey ST, Eeckhoute J, Cook J, Westerling T, et al. Growth factor stimulation induces a distinct ER(alpha) cistrome underlying breast cancer endocrine resistance. Genes Dev. 2011; 24:2219–27.
24. Tsai JH, Yang J. Epithelial-mesenchymal plasticity in carcinoma metastasis. Genes Dev. 2013; 27:2192–206. [PubMed: 24142872]
25. Lu J, Guo H, Treekitkarnmongkol W, Li P, Zhang J, Shi B, et al. 14-3-3zeta Cooperates with ErbB2 to promote ductal carcinoma in situ progression to invasive breast cancer by inducing epithelial-mesenchymal transition. Cancer Cell. 2009; 16:195–207. [PubMed: 19732720]
26. Rorth P. Collective cell migration. Annu Rev Cell Dev Biol. 2009; 25:407–29. [PubMed: 19575657]
27. Nishida N, Yano H, Nishida T, Kamura T, Kojiro M. Angiogenesis in cancer. Vasc Health Risk Manag. 2006; 2:213–9. [PubMed: 17326328]
28. Adams J, Carder PJ, Downey S, Forbes MA, MacLennan K, Allgar V, et al. Vascular endothelial growth factor (VEGF) in breast cancer: comparison of plasma, serum, and tissue VEGF and microvessel density and effects of tamoxifen. Cancer Res. 2000; 60:2898–905. [PubMed: 10850435]
29. Dalerba P, Cho RW, Clarke MF. Cancer stem cells: models and concepts. Annu Rev Med. 2007; 58:267–84. [PubMed: 17002552]
30. Kakarala M, Wicha MS. Implications of the cancer stem-cell hypothesis for breast cancer prevention and therapy. Journal Of Clinical Oncology: Official Journal Of The American Society Of Clinical Oncology. 2008; 26:2813–20. [PubMed: 18539959]
31. Pei XH, Bai F, Smith MD, Usary J, Fan C, Pai SY, et al. CDK inhibitor p18(INK4c) is a downstream target of GATA3 and restrains mammary luminal progenitor cell proliferation and tumorigenesis. Cancer Cell. 2009; 15:389–401. [PubMed: 19411068]
32. Ciarloni L, Mallepell S, Brisken C. Amphiregulin is an essential mediator of estrogen receptor alpha function in mammary gland development. Proc Natl Acad Sci U S A. 2007; 104:5455–60. [PubMed: 17369357]
33. Richards RG, Klotz DM, Walker MP, Diaugustine RP. Mammary gland branching morphogenesis is diminished in mice with a deficiency of insulin-like growth factor-I (IGF-I), but not in mice with a liver-specific deletion of IGF-I. Endocrinology. 2004; 145:3106–10. [PubMed: 15059953]
34. Murtaza M, Dawson SJ, Tsui DW, Gale D, Forshew T, Piskorz AM, et al. Non-invasive analysis of acquired resistance to cancer therapy by sequencing of plasma DNA. Nature. 2013; 497:108–12. [PubMed: 23563269]
35. Brooks MD, Burness ML, Wicha MS. Therapeutic Implications of Cellular Heterogeneity and Plasticity in Breast Cancer. Cell Stem Cell. 2015; 17:260–71. [PubMed: 26340526]
36. Asselin-Labat ML, Shackleton M, Stingl J, Vaillant F, Forrest NC, Eaves CJ, et al. Steroid hormone receptor status of mouse mammary stem cells. J Natl Cancer Inst. 2006; 98:1011–4. [PubMed: 16849684]
37. Fu N, Lindeman GJ, Visvader JE. The mammary stem cell hierarchy. Current topics in developmental biology. 2014; 107:133–60. [PubMed: 24439805]
38. Stingl J, Eirew P, Ricketson I, Shackleton M, Vaillant F, Choi D, et al. Purification and unique properties of mammary epithelial stem cells. Nature. 2006; 439:993–7. [PubMed: 16395311]

39. Schramek D, Leibbrandt A, Sigl V, Kenner L, Pospisilik JA, Lee HJ, et al. Osteoclast differentiation factor RANKL controls development of progestin-driven mammary cancer. Nature. 2010; 468:98–102. [PubMed: 20881962]
40. Rosen JM, Jordan CT. The increasing complexity of the cancer stem cell paradigm. Science. 2009; 324:1670–3. [PubMed: 19556499]
41. Kleinberg DL, Wood TL, Furth PA, Lee AV. Growth hormone and insulin-like growth factor-I in the transition from normal mammary development to preneoplastic mammary lesions. Endocr Rev. 2009; 30:51–74. [PubMed: 19075184]
42. Loladze AV, Stull MA, Rowzee AM, Demarco J, Lantry JH 3rd, Rosen CJ, et al. Epithelial-specific and stage-specific functions of insulin-like growth factor-I during postnatal mammary development. Endocrinology. 2006; 147:5412–23. [PubMed: 16901968]
43. Bonnette SG, Hadsell DL. Targeted disruption of the IGF-I receptor gene decreases cellular proliferation in mammary terminal end buds. Endocrinology. 2001; 142:4937–45. [PubMed: 11606462]
44. Creighton CJ, Casa A, Lazard Z, Huang S, Tsimelzon A, Hilsenbeck SG, et al. Insulin-like growth factor-I activates gene transcription programs strongly associated with poor breast cancer prognosis. J Clin Oncol. 2008; 26:4078–85. [PubMed: 18757322]
45. Fox EM, Miller TW, Balko JM, Kuba MG, Sanchez V, Smith RA, et al. A kinome-wide screen identifies the insulin/IGF-I receptor pathway as a mechanism of escape from hormone dependence in breast cancer. Cancer Res. 2011; 71:6773–84. [PubMed: 21908557]
46. Yee D. Insulin-like growth factor receptor inhibitors: baby or the bathwater? J Natl Cancer Inst. 2012; 104:975–81. [PubMed: 22761272]
47. Canzian F, McKay JD, Cleveland RJ, Dossus L, Biessy C, Rinaldi S, et al. Polymorphisms of genes coding for insulin-like growth factor 1 and its major binding proteins, circulating levels of IGF-I and IGFBP-3 and breast cancer risk: results from the EPIC study. Br J Cancer. 2006; 94:299–307. [PubMed: 16404426]
48. Robertson JF, Ferrero JM, Bourgeois H, Kennecke H, de Boer RH, Jacot W, et al. Ganitumab with either exemestane or fulvestrant for postmenopausal women with advanced, hormone-receptor-positive breast cancer: a randomised, controlled, double-blind, phase 2 trial. Lancet Oncol. 2013; 14:228–35. [PubMed: 23414585]

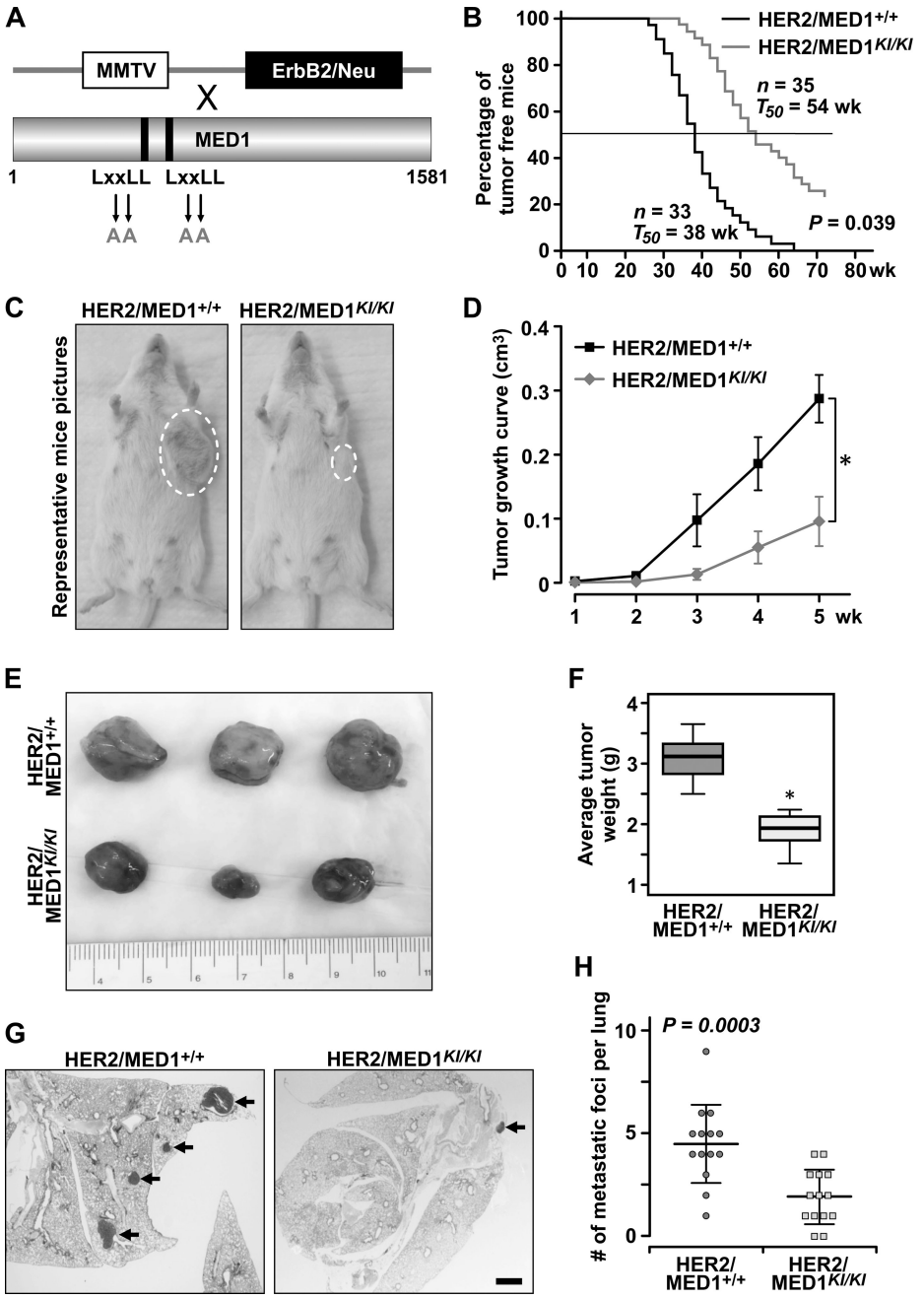

Fig 1. MED1$^{KI/KI}$ mutation impairs MMTV-HER2 mammary tumorigenesis

(A) Schematic representation of generation of MMTV-HER2/MED1$^{KI/KI}$ mice by crossing MMTV-HER2 and MED1$^{KI/KI}$ mice. (B) Kaplan-Meier analysis of tumor onsets with the median tumor free value T_{50} in MMTV-HER2/MED1$^{+/+}$ and MMTV-HER2/MED1$^{KI/KI}$ groups. (C) Representative image of MMTV-HER2/MED1$^{+/+}$ and MMTV-HER2/MED1$^{KI/KI}$ mice at the age of 40 weeks old. (D) Growth curves of MMTV-HER2/MED1$^{+/+}$ and MMTV-HER2/MED1$^{KI/KI}$ tumors. (E) Representative tumor pictures from MMTV-HER2/MED1$^{+/+}$ and MMTV-HER2/MED1$^{KI/KI}$ mice at the time of collection (2 months post palpation of primary tumors). (F) Quantification of tumor weight in MMTV-HER2/

MED1$^{+/+}$ and MMTV-HER2/MED1$^{KI/KI}$ groups. (G–H) H&E staining analyses of tumor lung metastasis in MMTV-HER2/MED1$^{+/+}$ (n=14) and MMTV-HER2/MED1$^{KI/KI}$ (n=14) mice (G) and the quantification (H). Bar = 1 mm.

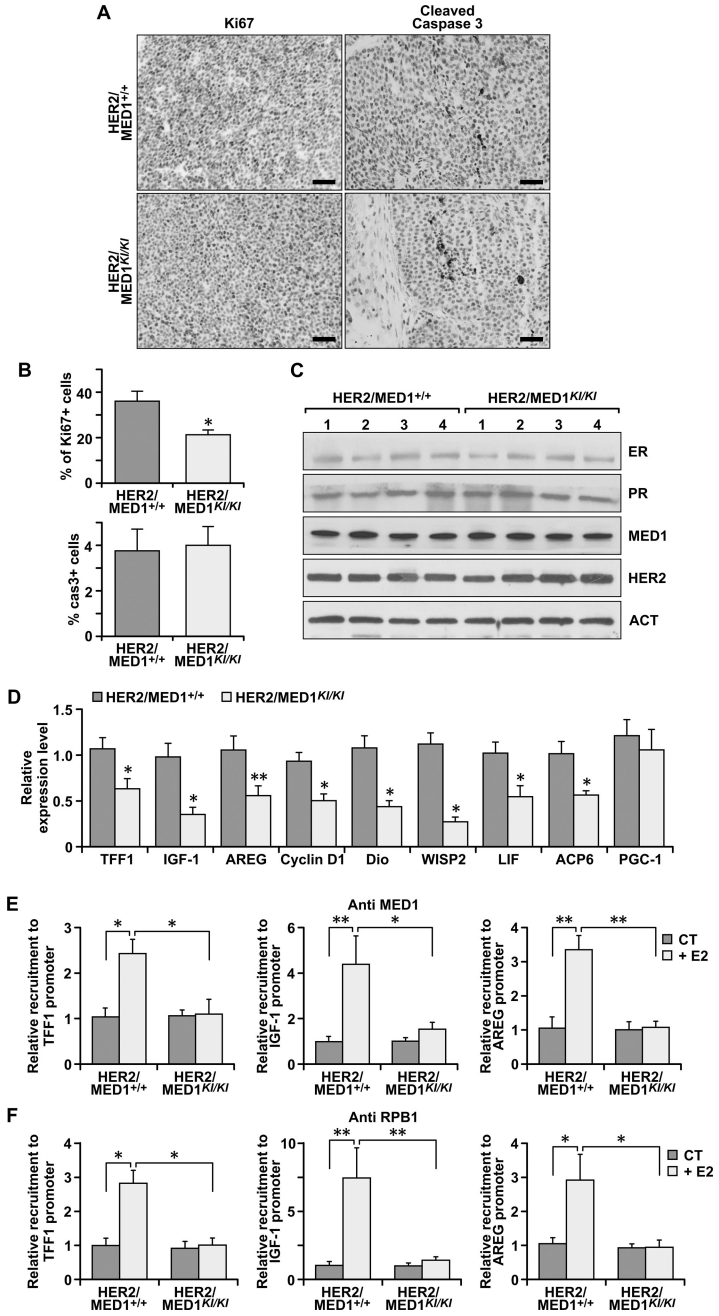

Fig 2. MMTV-HER2/MED1$^{KI/KI}$ mammary tumors exhibited decreased cell proliferation, increased necrosis and impaired ER target gene expression

(A–B) IHC staining of Ki67 and cleaved caspase-3 expression in MMTV-HER2/MED1$^{+/+}$ and MMTV-HER2/MED1$^{KI/KI}$ tumor sections (A) and quantifications of Ki67 and caspase-3 positive cells (B). Bar = 50 μm. (C) Immunoblotting analyses of the expression of ERα, PR, MED1, HER2 and Actin proteins in MMTV-HER2/MED1$^{+/+}$ and MMTV-HER2/MED1$^{KI/KI}$ tumors. (D) Relative mRNA level of indicated ER-target genes in MMTV-HER2/MED1$^{+/+}$ and MMTV-HER2/MED1$^{KI/KI}$ tumors by realtime RT-PCR analyses. (E–F) ChIP analyses of the occupancy of MED1 (E) and RNA polymerase II subunit I (RPB I) (F) on the promoter region of *TFF1, IGF-1* and *AREG* genes in MMTV-HER2/MED1$^{+/+}$ and

MMTV-HER2/MED1$^{KI/KI}$ tumor cells. The values are obtained in three independent experiments and shown as mean ± SD. *$P < 0.05$ or **$P < 0.01$.

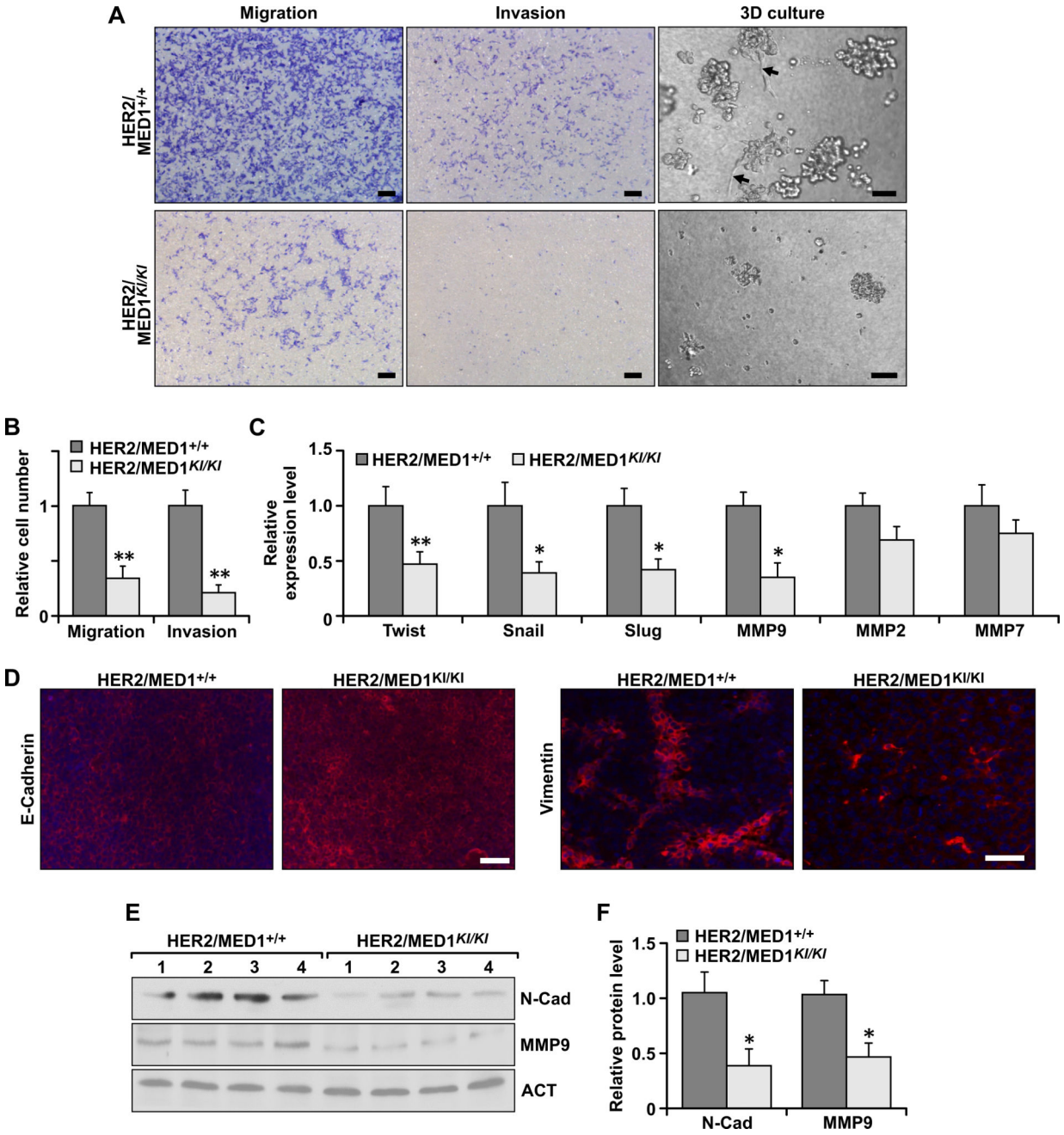

Fig 3. MED1 LxxLL motif mutations impaired migration, invasion and EMT of MMTV-HER2 tumors

(A) Tanswell assays (left two panels) and 3D culture (right panel) analyses of MMTV-HER2/MED1$^{+/+}$ and MMTV-HER2/MED1$^{KI/KI}$ tumor cells. (B) Quantification of relative migrated and invaded cells in (A). (C) Realtime RT-PCR analyses of the expression of indicated EMT-related genes in MMTV-HER2/MED1$^{+/+}$ and MMTV-HER2/MED1$^{KI/KI}$ tumors. (D) Immunofluorescence analyses of E-cadherin (left two panels) and Vimentin (right two panels) in the MMTV-HER2/MED1$^{+/+}$ and MMTV-HER2/MED1$^{KI/KI}$ tumors sections. (E–F) Immunoblotting analyses of N-cadherin and MMP9 proteins in MMTV-HER2/MED1$^{+/+}$ and MMTV-HER2/MED1$^{KI/KI}$ tumors (E) and quantification (F). The

values are obtained in three independent experiments and shown as mean ± SD. Bar = 100μm.*$P < 0.05$ or **$P < 0.01$.

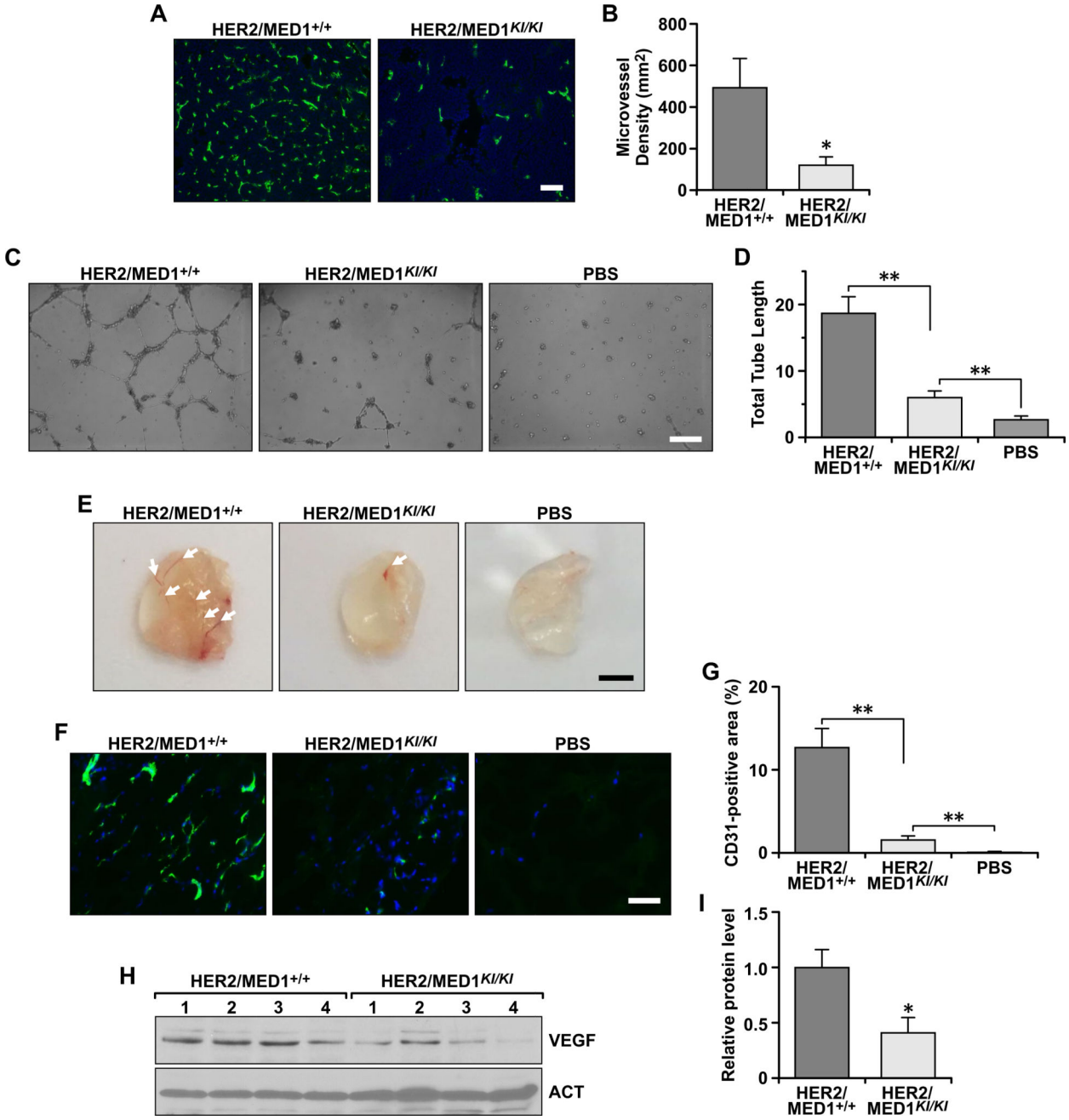

Fig 4. MED1 LxxLL motif mutations inhibited MMTV-HER2 tumor angiogenesis

(A–B) Immunofluorescence staining analyses of blood vessel marker CD31 protein expression in the MMTV-HER2/MED1$^{+/+}$ and MMTV-HER2/MED1$^{KI/KI}$ tumor sections (A) and statistical analyses of microvessel density (B). Bar = 100 μm. (C) *In vitro* microvessel formation assays using HUVECs treated with PBS control or conditioned medium from cultured MMTV-HER2/MED1$^{+/+}$ and MMTV-HER2/MED1$^{KI/KI}$ tumor cells. (D) Statistical analyses of the average tube length in each field. Bar = 100 μm. (E) Representative images of Matrigel plugs treated with control or conditioned medium from MMTV-HER2/MED1$^{+/+}$ and MMTV-HER2/MED1$^{KI/KI}$ tumor cells. Arrow pointed to the

formed blood vessels in the Matrigel plug *in vivo*. (F) Immunofluorescence analyses of CD31-positive blood vessel endothelial cells in the frozen sections of Matrigel plugs in (E). (G) Qualification of CD31-positive area in (F). (H–I) Western blots analyses of VEGF protein in MMTV-HER2/MED1$^{+/+}$ and MMTV-HER2/MED1$^{KI/KI}$ tumor cells (H) and qualification (I). The values are obtained in three independent experiments and shown as mean ± SD. *$P < 0.05$ or **$P < 0.01$.

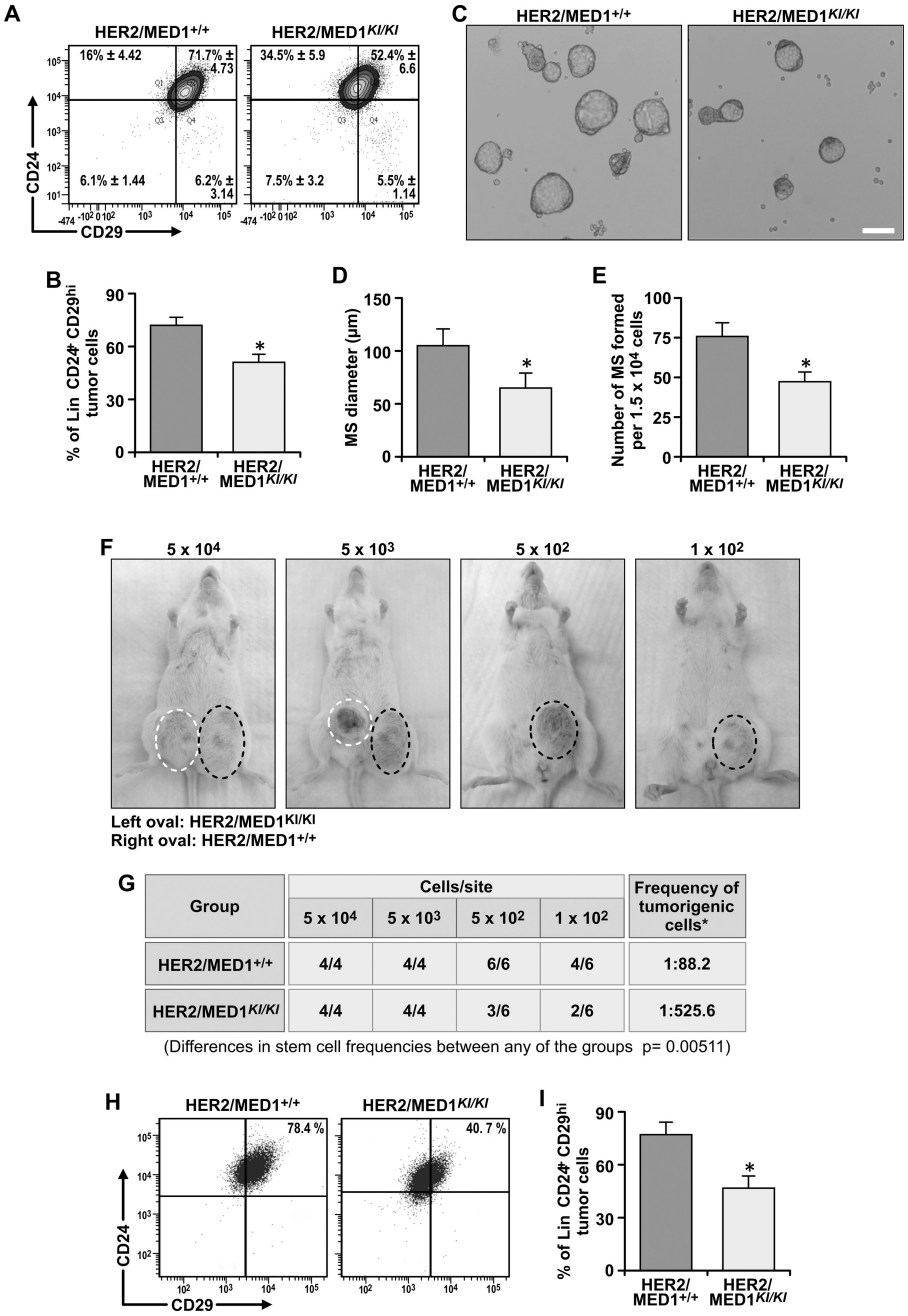

Group	Cells/site				Frequency of tumorigenic cells*
	5 x 10⁴	5 x 10³	5 x 10²	1 x 10²	
HER2/MED1+/+	4/4	4/4	6/6	4/6	1:88.2
HER2/MED1KI/KI	4/4	4/4	3/6	2/6	1:525.6

(Differences in stem cell frequencies between any of the groups p= 0.00511)

Fig 5. MED1 LxxLL motif mutations impaired MMTV-HER2 cancer stem cell formation and function both *in vitro* and *in vivo*

(A–B) Flow cytometry analyses of $Lin^{-}CD24^{+}CD29^{hi}$ CSCs enriched population in MMTV-HER2/MED1$^{+/+}$ and MMTV-HER2/MED1$^{KI/KI}$ primary tumors (A) and quantification (B). (C) Mammosphere formation assays using the same number of above FACS sorted cells (D–E) Quantification of the size (D) and member (E) of mammospheres formed in (C). (F) Representative tumor bearing NOD-SCID mice at 3month post orthotopic transplantation of indicated number (labeled above) of MMTV-HER2/MED1$^{KI/KI}$ (blue circle) and MMTV-HER2/MED1$^{+/+}$ (red circle) tumor cells. (G) Statistical analyses of tumor formation in each group of (F). (H–I) Flow cytometry analysis of $Lin^{-}CD24^{+}CD29^{hi}$ CSCs enriched

population in orthotopically xenografted tumors (H) and quantification (I). Bar = 100 μm. The values are obtained from three independent experiments and shown as mean ± SD. $*P < 0.05$ or $**P < 0.01$.

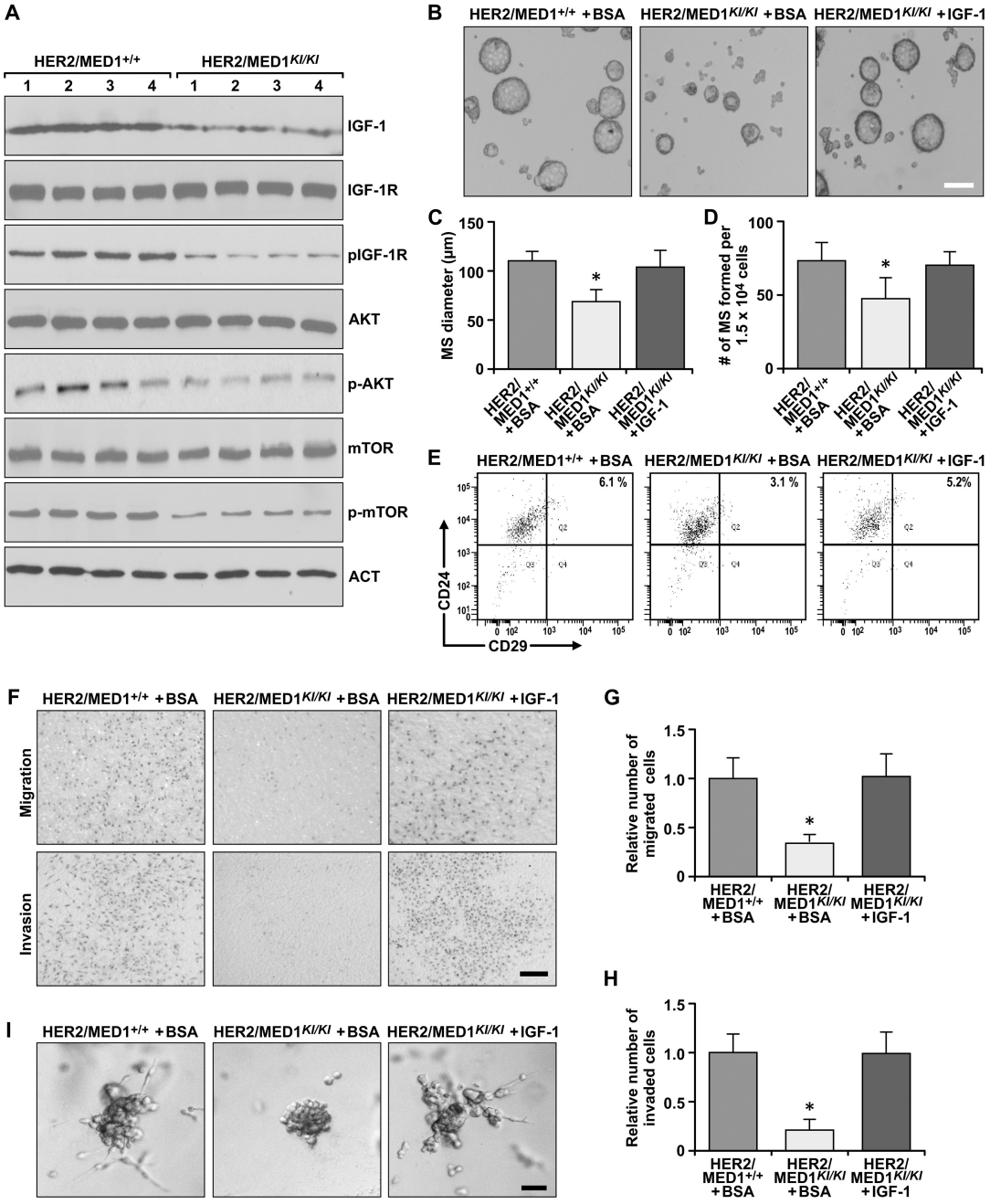

Fig 6. Exogenous IGF-1 rescues metastatic and mammosphere formation of MMTV-HER2/MED1$^{KI/KI}$ tumor cells *in vitro*

(A) Immunoblotting analyses of the expression and status of IGF-1 and its downstream signaling pathway components in MMTV-HER2/MED1$^{+/+}$ and MMTV-HER2/MED1$^{KI/KI}$ tumors. (B) Mammosphere formation assays using FACS sorted MMTV-HER2/MED1$^{+/+}$ and MMTV-HER2/MED1$^{KI/KI}$ tumor cells in the presence of BSA or IGF-1. Bar = 100 μm. (C–D) Average diameters (C) and numbers (D) of mammospheres formed in (B). (E) Flow cytometry analyses of CD24^{+}CD29^{hi} CSCs in the mammospheres of (B). (F) Transwell assays using MMTV-HER2/MED1$^{+/+}$ and MMTV-HER2/MED1$^{KI/KI}$ tumor cells in the presence of BSA or IGF-1. (G–H) Quantification of relative number of migrated (G) and

invaded (H) cells in (F). (I) 3D culture of MMTV-HER2/MED1$^{+/+}$ and MMTV-HER2/MED1$^{KI/KI}$ tumor cells in the presence of IGF-1 or BSA. Bar = 20 μm. The values are obtained in three independent experiments and shown as mean ± SD. *$P < 0.05$ or **$P < 0.01$.

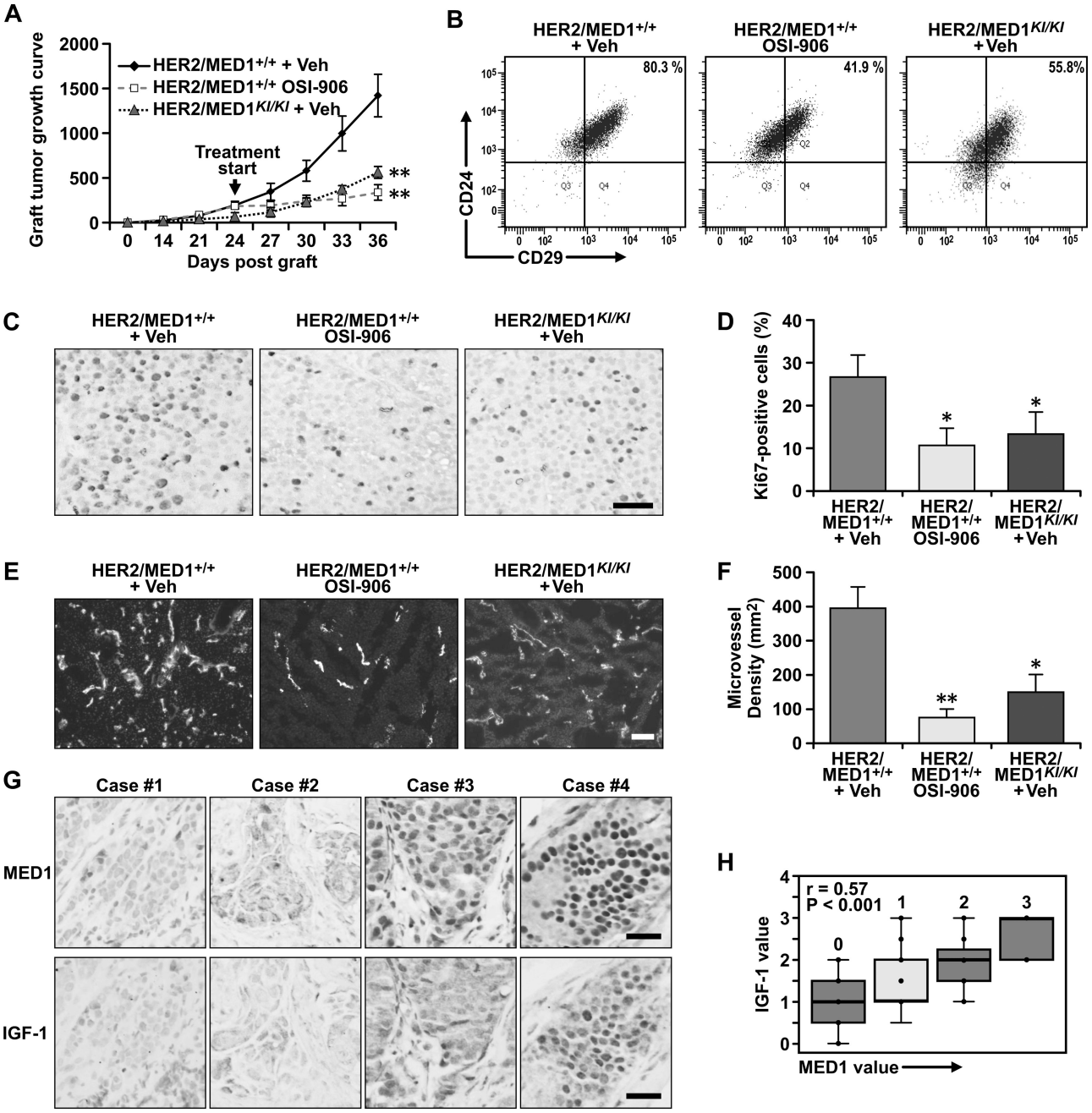

Fig 7. Inhibition of IGF-1 signaling phenocopies MED1$^{KI/KI}$ mutation in MMTV-HER2 tumors *in vivo*

(A) Growth curves of MMTV-HER2/MED1$^{+/+}$ and MMTV-HER2/MED1$^{KI/KI}$ grafted tumors treated with IGF-1R inhibitor OSI-906 or Vehicle control. (B) Flow cytometry analyses of Lin^{-}CD24^{+}CD29^{hi} CSCs enriched populations of the above tumors. (C–D) Immunostaining analyses of Ki67+ cells of the tumors sections (C) and quantifications (D). (E–F) Immunostaining analyses of CD31+ area in the sections of indicated tumors (E) and quantifications (F). (G) Representative immunocytochemical analyses of the expression of MED1 and IGF-1 in the sections of clinical breast cancer samples. (H) Correlation of MED1

with IGF-1 proteins level in clinical samples (n=76). Bar = 50 μm. The values are obtained in three independent experiments and shown as mean ± SD. *$P < 0.05$ or **$P < 0.01$.